

Microstructures of BaTiO₃ based PTC thermistors with Ca, Sr and Pb additions

L. Affleck, C. Leach*

Manchester Materials Science Centre
University of Manchester and UMIST
Grosvenor Street, Manchester M1 7HS, UK

Abstract

BaTiO₃ based PTC thermistors undergo a large and rapid increase in resistance just above the Curie temperature, T_C . The resistance increase is predominantly associated with an increase in grain boundary barrier height, therefore it is important to gain information about the grain boundary character in these devices. In this study the microstructures of three different BaTiO₃ PTC thermistor formulations were compared by transmission electron microscopy. The samples differed in the A-site substitutions, giving the formulae: (1) BaTiO₃, (2) (Ba,Ca)TiO₃, (3) (Ba,Ca,Sr,Pb)TiO₃. No grain boundary films were observed, though rounding of the grains at the grain junctions was evidence of a liquid second phase being present during sintering. EDX measurements were made across grain boundaries but no significant segregation of elements to the boundaries was observed.

Keywords: Electron microscopy, Grain boundaries, Microstructure – final, PTC devices, BaTiO₃ and titanates.

* Corresponding author. Email address: colin.leach@man.ac.uk

1. Introduction

PTC thermistors such as donor-doped BaTiO₃ undergo a large and rapid increase in resistance just above the Curie temperature, T_C . A-site substitutions of Sr or Pb are commonly added to control the switching temperature T_C .¹ Ca may also be added for a grain-refining effect.²

The PTC effect is attributed to an increase in the potential barrier height at the grain boundaries. The potential barrier has been attributed to the effects, both of a 2D layer of acceptor states and a thin insulating layer at the grain boundary.³ The model of a 2D layer of acceptor states at the grain boundary does not need a second phase film to be present. The model of a thin insulating layer at the grain boundary was developed because some experimental current-voltage data did not fit with the idea of a 2D layer of acceptor states.³ The thin insulating layer model requires the presence of a second phase film at the grain boundaries.

Grain boundary films are common in ceramics, particularly at high angle grain boundaries, since wetting can lower the grain boundary energy. Grain boundary films or intergranular layers of a second phase have been predicted by some authors to give a better fit to the measured current-voltage data than is possible without such a layer.^{4,5} Gerthsen and Hoffmann⁴ proposed a 600 nm thick layer of TiO₂-rich second phase at the grain boundaries of BaTiO₃, while Hayashi *et al*⁵ proposed a 100 nm thick layer of BaTiO₃ with acceptor point defects at the grain boundaries. However, most studies of the microstructure of barium titanate by transmission electron microscopy (TEM), to a resolution of 2-10 nm, did not show the presence of any grain boundary films or intergranular layers of a second phase.^{6,7} There has been only one reported TEM observation of such a layer at the grain boundaries.⁸

Evidence for the 2D layer of acceptor states model would include segregation of acceptor atoms to the grain boundaries. Segregation of elements such as Fe to the grain boundaries has been observed by STEM in conjunction with energy-dispersive X-ray analysis (EDAX).⁷

In this study the microstructures of grain boundaries in thermistor formulations with differing compositions are compared, using TEM and SEM, to characterise the influence of A-site substitutions on grain boundary character.

2. Experimental

Commercial donor-doped BaTiO₃ pellets were supplied by GE Thermometrics (UK) Ltd in three different formulations based on BaTiO₃, (Ba,Ca)TiO₃ and (Ba,Ca,Sr,Pb)TiO₃. The pellets were prepared by sintering at a peak temperature of 1300°C.

Thin specimens were prepared for analysis by TEM, by grinding, cutting and mounting onto a Cu grid, followed by dimpling and ion beam thinning. A Philips CM200 TEM, fitted with an EDAX energy-dispersive X-ray spectrometer, was used to analyse the microstructure and composition of the specimens. A FEI Tecnai F30 FEGTEM/STEM fitted with an EDAX spectrometer was used to obtain compositional linescan information across a grain boundary. Thermistor pellets were also polished with colloidal silica in order to obtain orientation contrast in backscattered electron images, using a Philips XL30 FEGSEM.

3. Results and Discussion

3.1. Second phases

A crystalline, untwinned second phase was seen in all the samples (Figure 1). It was located at triple junctions, and varied in width from a few nm to 2 μm . The second phase contained Ba, Ti, O and reduced levels of dopants. It was silicon-rich ($\sim 16\%$) in all samples, except for the $(\text{Ba,Ca})\text{TiO}_3$ formulation where it was just composed of Ba, Ti and O. In this sample, Ca was only detected within the grains and Si was not detected at all.

The angle that the second phase makes with the grains can provide information about wetting behaviour. For a grain boundary to be wet by a second phase, the dihedral angle, Φ , must be less than 60° . TEM micrographs of the second phases at grain junctions in the samples studied here show a range of dihedral angles, mainly from $\sim 30^\circ$ to 50° , although a few larger angles were noted. This suggests that in most cases grain boundary wetting should occur, i.e. a layer of second phase should be seen at the interface between two grains.

3.2. Grain boundary films

No grain boundary films thicker than 50 nm were observed in any of the samples (Figure 2). Some rounding of grains at the grain junctions was observed, however, which was evidence of a liquid grain boundary phase being present during sintering (Figure 1). It is possible that some grain boundaries were wetted at high temperatures during sintering, but de-wetted upon cooling. Previous studies on the role of sintering aids in BaTiO_3 thermistors have inferred the presence of a liquid phase around the grains at the sintering temperature, but that this accumulates at grain junctions upon cooling leaving boundaries virtually free of second phase.⁹

3.3. Segregation

A series of spot EDX analyses was made across a grain boundary in each sample, to determine whether any segregation of elements to the boundary could be detected. The nanoprobe TEM mode was used; the electron spot width for analysis was about 15 nm. A suitable grain boundary, that was parallel to the electron beam during analysis, was found in each sample. Spot analyses taken at the grain boundary interface and to either side showed no evidence for grain boundary segregation. Additionally a linescan across a grain boundary in a BaTiO₃ sample was performed, with analyses taken every 2 nm using a 2 nm spot size (Figure 3). The line in Figure 3(a) shows the position of the grain boundary. Again, no evidence for grain boundary segregation was observed. It was concluded that, in the samples studied here, any segregation of elements to the grain boundary was below the detectability limit of the EDAX detector (~0.5 %).

3.4. Twins

The microstructures of each barium titanate formulation show twinning in most grains (Figure 4). The width of the twin domains and the spacing between them was measured from TEM micrographs, with the twin planes oriented parallel to the electron beam. Generally the twins are between a few 10s and a few 100s of nanometres wide.

Figure 4(a) shows the twinning in the BaTiO₃ sample, in which many grains contained a double annealing twin (A), running across the grain. Such twins were not observed in the (Ba,Ca)TiO₃ and (Ba,Ca,Sr,Pb)TiO₃ samples, Figure 4(b) and (c). All of the samples had single annealing twins (B), straight parallel (ferroelectric) twins (C) and tapered (deformation) twins (D). The ferroelectric twin planes in each sample were indexed and found to be {101}, in common with other published data.¹⁰ In BaTiO₃, {101} twins form during the cubic to

tetragonal phase transformation, to release the induced stresses.¹¹ {111} annealing twins form during sintering and are associated with abnormal grain growth.¹¹

3.5. *Misoriented regions*

In the (Ba,Ca,Sr,Pb)TiO₃ sample, some grains contained small regions of about 1 μm diameter that were of a similar composition but slightly misoriented with respect to the surrounding grain. Figure 5 shows a TEM bright field image of such a misoriented, untwinned, region along with diffraction patterns from this region and the surrounding grain. The misorientation is described by a rotation of 5.1° in the plane of the sample and a 7.5° about an axis parallel to the electron beam. The interface with the host grain is sharp. The origin of these regions is currently uncertain and will be the subject of further study.

4. **Conclusions**

The microstructures of three different compositions of PTC thermistors based on BaTiO₃ with different A-site substitutions were compared by TEM and were found to be similar in many respects. No grain boundary film and no evidence for segregation of elements to the grain boundaries were observed in any of the samples. In the BaTiO₃ and (Ba,Ca,Sr,Pb)TiO₃ samples a crystalline Si-rich second phase was found at the junctions of rounded grains, implying that the second phase was liquid at the sintering temperature. All the samples had a spread of twin widths between a few 10s and a few 100s of nanometres wide. Ferroelectric, deformation and single annealing twins were observed in all samples. The BaTiO₃ sample also had double annealing twins. The (Ba,Ca,Sr,Pb)TiO₃ sample contained some misoriented regions that were not observed in the other compositions.

Acknowledgements

This work was funded through EPSRC grant number GR/R00500/01. GE Thermometrics (UK) Ltd are thanked for the supply of the thermistor pellets used in this study. Peter Kenway of the Manchester Materials Science Centre is thanked for his help with the TEM studies.

References

1. Hill, D. and Tuller, H., Ceramic Sensors: Theory and Practise. In *Ceramic Materials for Electronics*, (Ed. R. Buchanan), Marcel Dekker Inc, NY, 1991, p335.
2. Voltzke, D., Abicht, H., Pippel, E. and Woltersdorf, J., Ca-containing additives in PTC-BaTiO₃ ceramics: effects on the microstructural evolution. *J. Eur. Ceram. Soc.*, 2000, **20**, 1663-1669.
3. Daniels, J. and Wernicke, R., New aspects of an improved PTC model. *Philips Res. Repts.*, 1976, **31**, 544-559.
4. Gerthsen, P. and Hoffmann, B., Current-voltage characteristics and capacitance of single grain boundaries in semiconducting BaTiO₃ ceramics. *Solid State Electronics*, 1973, **16**, 617-622.
5. Hayashi, K., Yamamoto, T., Ikuhara, Y. and Sakuma, T., Grain boundary electrical barriers in positive temperature coefficient thermistors. *J. Appl. Phys.*, 1999, **86**, 2909-2913.
6. Hayashi, K., Yamamoto, T., Ikuhara, Y. and Sakuma, T., Formation of potential barrier related to grain-boundary character in semiconducting barium titanate. *J. Am. Ceram. Soc.*, 2000, **83**, 2684-2688.
7. Desu, S. and Payne, D., Interfacial Segregation in Perovskites: 2, Experimental Evidence. *J. Am. Ceram. Soc.*, 1990, **73**, 3398-3406.
8. Rehme, H., Imaging electric microfields in emission electron microscope. *Z. angew. Physik*, 1970, **29**, 173.
9. Cheng, H., Effect of sintering aids on the electrical properties of positive temperature coefficient of resistivity BaTiO₃ ceramics. *J. Appl. Phys.*, 1989, **66**, 1382-1387.

10. Hu, Y., Chan, H., Wen, Z. and Harmer, M., Scanning Electron Microscopy and Transmission Electron Microscopy Study of Ferroelectric Domains in Doped BaTiO₃. *J. Am. Ceram. Soc.*, 1986, **69**, 594-602.
11. Lee, B. and Kang, S., Second-phase assisted formation of {111} twins in barium titanate. *Acta Mater.*, 2001, **49**, 1373-1381.

List of figures

Figure 1. TEM micrographs of untwinned crystalline second phase in (a) (Ba,Ca,Sr,Pb)TiO₃ sample; (b) (Ba,Ca)TiO₃ sample. The insets show selected area electron diffraction patterns of each second phase region.

Figure 2. TEM micrograph of a grain boundary without a film, in a (Ba,Ca,Sr,Pb)TiO₃ sample.

Figure 3. (a) Plot of the amount of each element along a line across a grain boundary, in a BaTiO₃ sample. No segregation at a resolution of ~2 nm is observed. (b) STEM micrograph of the grain boundary showing the position of the linescan.

Figure 4. Backscattered electron micrographs of the barium titanate samples studied, showing twinning in the grains. (a) BaTiO₃, (b) (Ba,Ca)TiO₃, (c) (Ba,Ca,Sr,Pb)TiO₃. Arrows indicate twin types: A – double annealing twins, B – single annealing twins, C – parallel (ferroelectric) twins, D – tapered (deformation) twins. (Scale bars = 5 μm.)

Figure 5. TEM micrograph of misoriented region in (Ba,Ca,Sr,Pb)TiO₃ sample. Insets show selected area diffraction patterns of the region and surrounding grain with the same sample orientation.

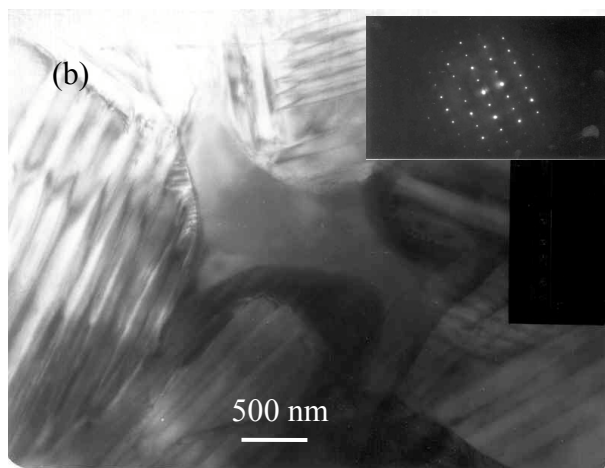
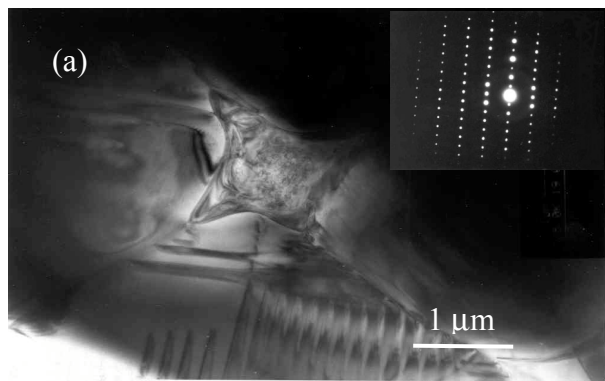


Figure 1. TEM micrographs of untwinned crystalline second phase in (a) $(\text{Ba,Ca,Sr,Pb})\text{TiO}_3$ sample; (b) $(\text{Ba,Ca})\text{TiO}_3$ sample. The insets show selected area electron diffraction patterns of each second phase region.

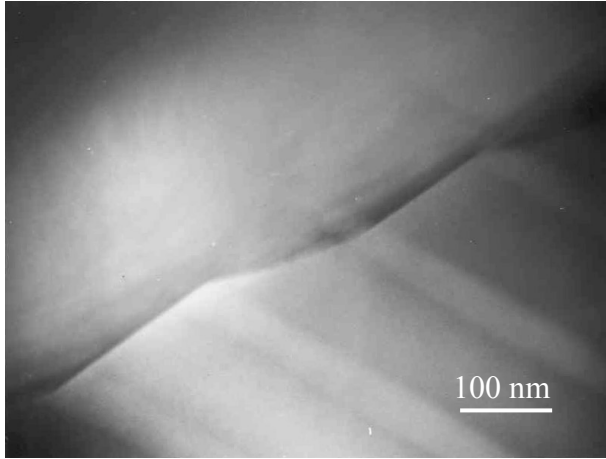


Figure 2. TEM micrograph of a grain boundary without a film, in a (Ba,Ca,Sr,Pb)TiO₃ sample.

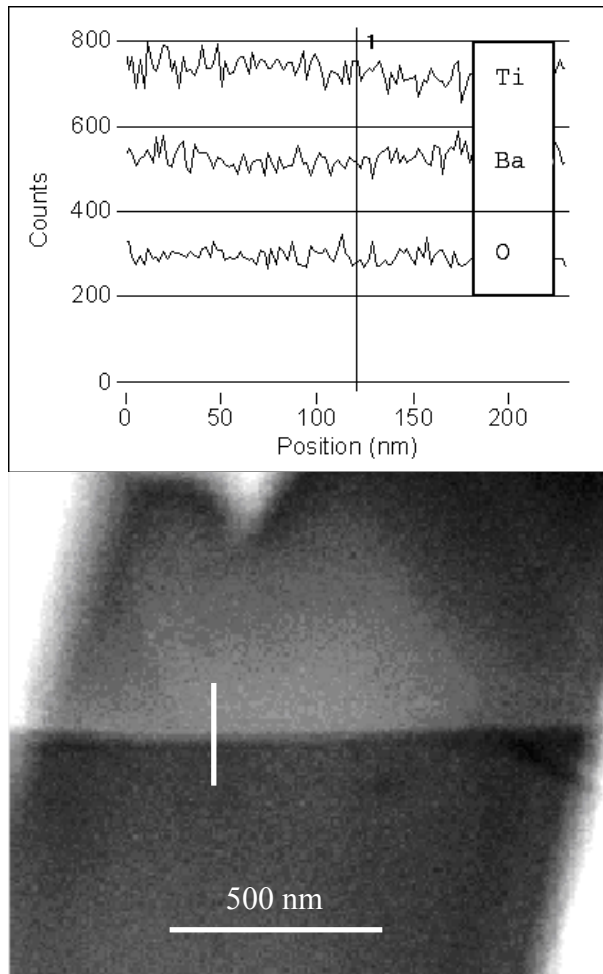


Figure 3. (a) Plot of the amount of each element along a line across a grain boundary, in a BaTiO₃ sample. No segregation at a resolution of ~2 nm is observed. (b) STEM micrograph of the grain boundary showing the position of the linescan.

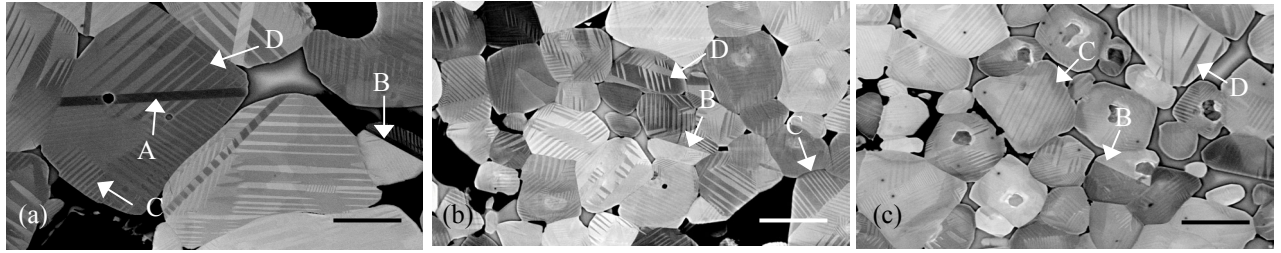


Figure 4. Backscattered electron micrographs of the barium titanate samples studied, showing twinning in the grains. (a) BaTiO_3 , (b) $(\text{Ba,Ca})\text{TiO}_3$, (c) $(\text{Ba,Ca,Sr,Pb})\text{TiO}_3$. Arrows indicate twin types: A – double annealing twins, B – single annealing twins, C – parallel (ferroelectric) twins, D – tapered (deformation) twins. (Scale bars = 5 μm .)

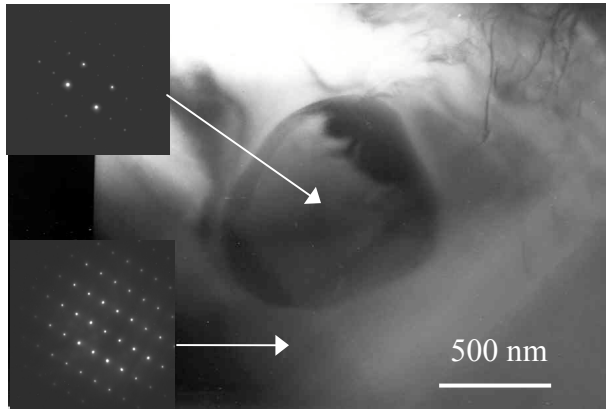


Figure 5. TEM micrograph of misoriented region in (Ba,Ca,Sr,Pb)TiO₃ sample. Insets show selected area diffraction patterns of the region and surrounding grain with the same sample orientation.